A FREQUENCY DOMAIN METHOD FOR REGISTRATION OF RANGE DATA

G.M. Cortelazzo, G. Doretto, L. Lucchese, S. Totaro

Department of Electronics and Informatics
University of Padova
Via Gradenigo 6/A, 35131, Padova, Italy
e-mail: {corte,doretto,lulaluc,tost}@dei.unipd.it

ABSTRACT

Free-form 3-D surfaces registration is a fundamental problem in 3-D imaging, tipically approached by extensions or variations of the ICP algorithm. This work presents an alternative method for 3-D motion estimation based on the Fourier transform of the range data. The frequency domain techniques for estimating motion parameters are non feature-based methods suitable for unsupervised registration of 3-D views. The proposed method can give unsupervised registration of range data within 1° of accuracy of the angular parameters, useful "per se" in applications where this kind of precisions is adeguate or which can serve as good starting point for the ICP algorithm when a higher precision is needed.

1. INTRODUCTION

Range data registration is tipically done by the ICP algorithm or its extensions [1, 2, 3]. This work shows how to apply in this task an algorithmic idea for 3-D motion estimation originally proposed in [4]. The proposed method works in the frequency domain and it inherits the robustness of similar approaches used in the 2-D case [5, 6]. Since our technique is not based on features it can become a tool for unsupervised registration of range data. The following section summarizes the algorithmic idea for estimating the rigid motion parameters. Section 3 discusses the performance and Section 4 has the conclusions.

2. RIGID MOTION ESTIMATION

Let $s_1(\mathbf{x})$, $\mathbf{x} \in I\!R^3$, be the range data of the surface of a 3-D object and let $s_2(\mathbf{x})$ be a rigidly translated and rotated version of $s_1(\mathbf{x})$, i.e.

$$s_2(\mathbf{x}) = s_1(R^{-1}\mathbf{x} - \mathbf{t})\,. \tag{1}$$

According to (1) $s_2(\mathbf{x})$ is first translated by the vector $\mathbf{t} \in I\!R^3$ and then rotated by the matrix[1] $R \in SO(3)$.

Range data of this kind are associated to two free-form 3-D objects taken from two arbitrary points of view, or, in the view registration problem; they may be obtained from the common part of two partially overlapped views of an object.
Denote as

$$\mathcal{S}_i(\mathbf{k}) \doteq \mathcal{F}[s_i(\mathbf{x}) \mid \mathbf{k}] = \iiint_{-\infty}^{+\infty} s_i(\mathbf{x}) e^{-j2\pi \mathbf{k}^T \mathbf{x}}\, d\mathbf{x}\,, \tag{2}$$

$$\mathbf{k} = \begin{bmatrix} k_x & k_y & k_z \end{bmatrix}^T\,,$$

the 3-D cartesian Fourier transform of $s_i(\mathbf{x}), i = 1, 2$; it is straightforward to prove that the two transforms are related as

$$\mathcal{S}_2(\mathbf{k}) = \mathcal{S}_1(R^{-1}\mathbf{k}) e^{-j2\pi \mathbf{k}^T R \mathbf{t}}\,. \tag{3}$$

Relationships (1) and (3) hold for 3-D surfaces as well as for 3-D solids. However, if the 3-D surfaces were modeled by impulsive functions supported on them, their Fourier transforms would have a lot of spurious high frequency content not suited to frequency domain methods. For this reason we preliminarily build 3-D solids from the range data defined by the 3-D surfaces as follows. The proposed way differs from that used in [4], which although effective is rather impractical for applicative purposes. The solids companion to the range surfaces are defined as

$$\ell_i(\mathbf{x}) = \int_S s_i(\mathbf{x} - \mathbf{y}) h(\mathbf{y})\, d\mathbf{y}\,, \qquad i = 1, 2\,, \tag{4}$$

with

$$h(\mathbf{y}) = \frac{1}{1 + \|\mathbf{y}\|_2}\,, \tag{5}$$

and S a small sphere centered around the origin. With the data we used, which typically were matrices $128 \times 128 \times 128$, taking S with 9 pixels diameter was found to be a good choice. Other choices for $h(\mathbf{y})$ and S would also be possible. The purpose of convolution (4) is to create small weighted solid regions around 3-D surface $s_i(\mathbf{x})$, with weight decreasing with the distance from $s_i(\mathbf{x})$. In this way solids $\ell_i(\mathbf{x})$ ideally maintain the same spatial information of the 3-D surfaces $s_i(\mathbf{x})$, without the mathematical difficulties associated to their impulsive supports. Fig.1-(a) shows a view of the range data surface $s_1(\mathbf{x})$ (namely the file `FACE35` of [7]) and Fig.1-(c) a view of its companion solids $\ell_1(\mathbf{x})$ defined by (4). Similar views for the range surface `JET1` of [7] and its companion solids are shown by Fig.1-(b) and Fig.1-(d) respectively.

This work was partially supported by CNR Progetto Finalizzato Beni Culturali.

[1] $SO(3) = \{R \in I\!R^{3\times 3}, R^{-1} = R^T, \det(R) = +1\}$ is the group of the 3×3 special orthogonal matrices.

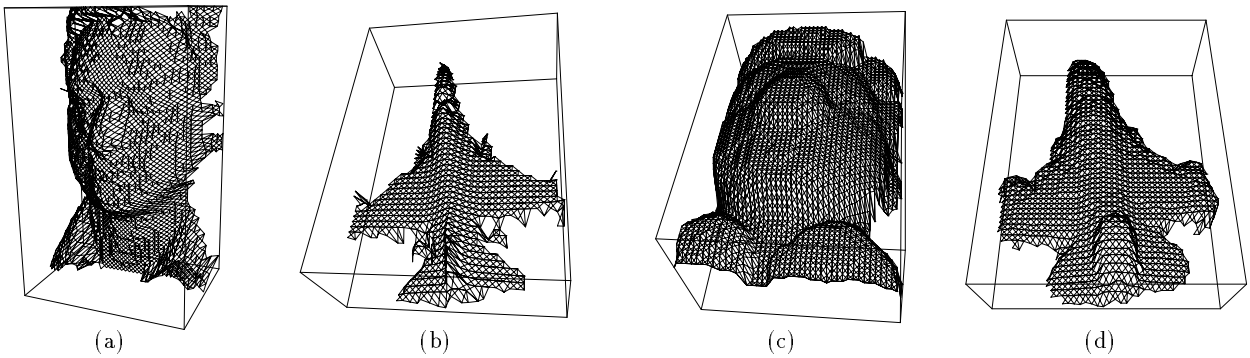

(a) (b) (c) (d)

Figure 1: Range images FACE35 (a) and JET1 (b) of [7]; (b)-(c) companion solids.

The Fourier transforms of $\ell_i(\mathbf{x})$, $i = 1, 2$, defined as $\mathcal{L}_i(\mathbf{k}) \doteq \mathcal{F}[\ell_i(\mathbf{x}) \mid \mathbf{k}]$, $i = 1, 2$, from (2), satisfy (3) like $\mathcal{L}_i(\mathbf{k})$, $i = 1, 2$.

With reference to $\mathcal{L}_i(\mathbf{k})$, $i = 1, 2$, from (3) it can be noticed that the translational vector $\mathbf{t}$ affects only phases and not magnitudes. Therefore the magnitudes are related as

$$|\mathcal{L}_2(\mathbf{k})| = |\mathcal{L}_1(R^{-1}\mathbf{k})| \,. \tag{6}$$

Relationship (6) can be used in order to determine R. In fact in the frequency domain the estimation of R and $\mathbf{t}$ can be decoupled and one can estimate first R from (6) and then $\mathbf{t}$ from (3).

The algorithm is summarized below. Further details can be found in [4].

2.1. *Estimate of the rotational axis ω*

Define the difference function $\mathcal{Q}(\mathbf{k})$ between the transforms magnitudes as

$$\mathcal{Q}(\mathbf{k}) \doteq \left| \frac{|\mathcal{L}_1(\mathbf{k})|}{\mathcal{L}_1(\mathbf{0})} - \frac{|\mathcal{L}_2(\mathbf{k})|}{\mathcal{L}_2(\mathbf{0})} \right| = \left| \frac{|\mathcal{L}_1(\mathbf{k})|}{\mathcal{L}_1(\mathbf{0})} - \frac{\left|\mathcal{L}_1(R^{-1}\mathbf{k})\right|}{\mathcal{L}_1(\mathbf{0})} \right| , \tag{7}$$

where relationship (5) has been used. From (7) it is clear that $\mathcal{Q}(\mathbf{k}) = 0$ if $R^{-1}\mathbf{k} = \mathbf{k}$ which is equivalent to $R\mathbf{k} = \mathbf{k}$. It can be straightforwardly proved that the rotational matrix R possesses the eigenvalues $\lambda_1 = 1$, $\lambda_2 = e^{j\psi}$ and $\lambda_3 = e^{-j\psi}$, where ψ is the angular shift around the rotation axis corresponding to R. If ω denotes the unit vector pointing towards the same direction of the rotation axis, it can be proved that ω has the following properties: i) it is the eigenvector associated to $\lambda_1 = 1$ (therefore it satisfies $R\mathbf{k} = \mathbf{k}$); ii) it is the only real eigenvector of R. In other words the locus $\mathcal{Q}(\mathbf{k}) = 0$ includes a line through ω. For objects without special symmetries (as natural objects typically are) this property of the function $\mathcal{Q}(\mathbf{k})$ can be exploited in order to determine the versor ω through the following procedure:

1) express $\mathcal{Q}(k_x, k_y, k_z)$ in spherical coordinates as $\overline{\mathcal{Q}}(k_\rho, k_\varphi, k_\theta)$; notice that this function can be represented only in a hemisphere because of the hermitian symmetry of the Fourier transform;

2) compute the radial projection of $\overline{\mathcal{Q}}(k_\rho, k_\varphi, k_\theta)$ as

$$\mathcal{P}(k_\varphi, k_\theta) \doteq \int_0^\infty \overline{\mathcal{Q}}(k_\rho, k_\varphi, k_\theta)\, dk_\rho \,; \tag{8}$$

3) the angular coordinates of ω in spherical representation can be found as

$$(\varphi, \theta) = \arg \min_{k_\varphi, k_\theta} \left[\mathcal{P}(k_\varphi, k_\theta)\right] , \tag{9}$$

since, from the inclusion of ω within the locus $\mathcal{Q}(\mathbf{k}) = 0$, $\mathcal{P}(k_\varphi, k_\theta) \geq 0$ with $\mathcal{P}(\varphi, \theta) = 0$;

4) define ω the versor of the direction (φ, θ).

The use of radial projections (7) simplifies the 3-D search for a line of the locus $\mathcal{Q}(\mathbf{k}) = 0$ into the minimization of a 2-D function which can be solved by standard numerical methods.

2.2. *Estimate of the rotational angle ψ*

Once the rotational axis ω has been determined, the estimate of the rotational angle ψ can be conveniently approached in a cilindrical coordinate system (u, v, w) with the w-axis along ω. In this new reference system the 3-D rotation matrix $R_w(\psi)$ clearly shows the structure of a rotation by ψ around the w-axis, i.e., it becomes

$$R_w(\psi) = \begin{bmatrix} \cos\psi & -\sin\psi & 0 \\ \sin\psi & \cos\psi & 0 \\ 0 & 0 & 1 \end{bmatrix} \doteq \left[\begin{array}{cc|c} & & 0 \\ \multicolumn{2}{c|}{r(\psi)} & 0 \\ \hline 0 & 0 & 1 \end{array}\right] . \tag{10}$$

If the magnitudes (6) are projected along the w-axis as

$$p_i(u, v) = \int_{-\infty}^{+\infty} |\bar{\mathcal{L}}_i(u, v, w)|\, dw \qquad i = 1, 2 \,, \tag{11}$$

it is

$$p_2\left(\begin{bmatrix} u \\ v \end{bmatrix}\right) = p_1\left(r^{-1}(\psi)\begin{bmatrix} u \\ v \end{bmatrix}\right) . \tag{12}$$

and the determination of ψ from (12) can be solved by the technique of [5] since it is a 2-D rotation estimate. The disambiguation between the two admissible estimates $\widehat{\psi}$ and $\widehat{\psi} + \pi$, due to the hermitian symmetry of the Fourier transform, can be accomplished along with the estimate of the translational vector $\mathbf{t}$ (see [6]) by means of the following procedure.

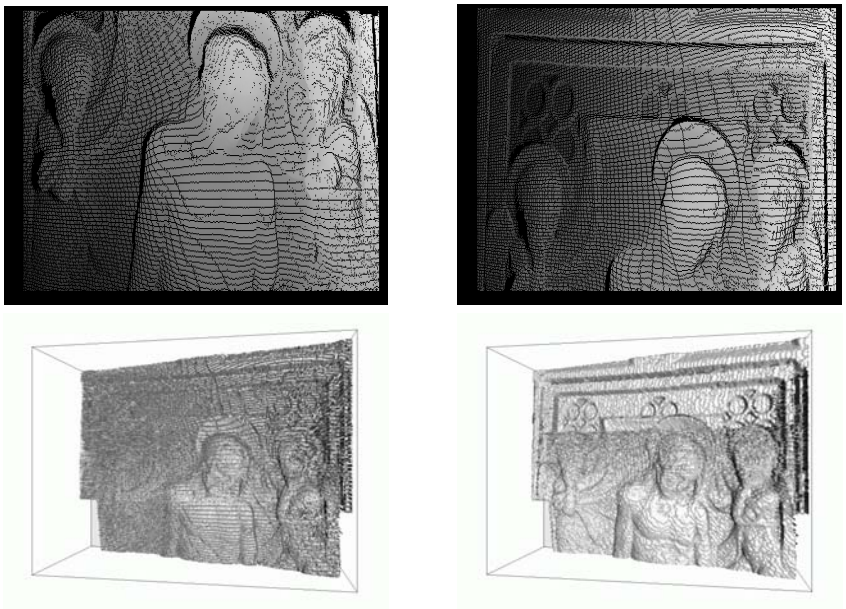

Figure 2: (a), (b) views of partial range images[2]; (c) view of straight composition; (d) view of composition after pre-filtering.

2.3. *Estimate of the translational vector* $\mathbf{t}$

The translational vector $\mathbf{t}$ can be estimated as follows [6]:

a) de-rotate the image $l_2(\mathbf{x})$ as

$$d_2(\mathbf{x}) = l_2(R\mathbf{k}) = l_1(\mathbf{x} - \mathbf{t}) \; ; \qquad (13)$$

b) apply a 3-D cartesian phase correlation algorithm on $\mathcal{L}_1(\mathbf{k})$ and $\mathcal{D}_2(\mathbf{k}) \doteq \mathcal{F}[d_2(\mathbf{x}) \mid \mathbf{k}] = \mathcal{L}_1(\mathbf{k})\; e^{-j2\pi\mathbf{k}^T\mathbf{t}}$, i.e., compute the normalized product between transforms as

$$\Gamma(\mathbf{k}) \doteq \frac{\mathcal{L}_1^*(\mathbf{k})\mathcal{D}_2(\mathbf{k})}{|\mathcal{L}_1(\mathbf{k})\mathcal{D}_2(\mathbf{k})|} = e^{-j2\pi\mathbf{k}^T\mathbf{t}} \; ; \qquad (14)$$

c) evaluate its inverse Fourier transform

$$\gamma(\mathbf{x}) \doteq \mathcal{F}^{-1}[\Gamma(\mathbf{k}) \mid \mathbf{x}] = \delta(\mathbf{x} - \mathbf{t}) \; . \qquad (15)$$

The translational vector $\mathbf{t}$ can be estimated from the peak of the 3-D impulsive function $\gamma(\mathbf{x})$. The method can be efficiently implemented by using MD-FFT algorithms [8, 9].

3. EXPERIMENTAL RESULTS AND DISCUSSION

In order to test the performance of the proposed algorithm, a number of range images from [7] were rotated about known quantities (φ, θ, ψ) whose values $(\hat{\varphi}, \hat{\theta}, \hat{\psi})$ were estimated by the algorithm. The results of these tests are exemplified by Table 1 and 2.

Table 1 reports the performance concerning the range image of Fig.1-(a). The angular parameters are generally estimated within 1° of accuracy, and in one case (test 3) φ is estimated with an accuracy of 2°.

Table 2 shows the performance of the algorithm with the range image of Fig.1-(b). The angular parameters are typically estimated within 1.5° of accuracy, except for test 6 where $\hat{\theta}$ is estimated with an error of 3.5°.

TEST	TRUE			ESTIMATED		
	φ	θ	ψ	$\hat{\varphi}$	$\hat{\theta}$	$\hat{\psi}$
1	90.0	0.0	-25.0	89.0	-0.5	-24.25
2	15.0	30.0	40.0	15.5	31.0	40.75
3	60.0	20.0	15.0	62.0	20.0	14.25
4	10.0	30.0	20.0	9.5	30.0	20.60

Table 1: Results about `FACE35` [7].

TEST	TRUE			ESTIMATED		
	φ	θ	ψ	$\hat{\varphi}$	$\hat{\theta}$	$\hat{\psi}$
1	40.0	5.0	35.0	40.5	4.0	34.25
2	14.0	8.0	18.0	12.5	7.5	19.00
3	4.0	25.0	20.0	7.0	26.5	18.25
4	40.0	13.0	37.0	39.5	14.0	37.00
5	40.0	13.0	5.0	39.5	13.5	4.68
6	90.0	0.0	-25.0	91.0	-3.5	-23.50

Table 2: Results about `JET1` [7].

These results refer to the use of the algorithm in a "single shot", as explained in Section 2. However, it is important to point out that estimates of φ and θ with at most one degree of accuracy are always present among the lowest (three or four) local minima of $\mathcal{P}(k_\varphi, k_\theta)$ (the estimate of φ and θ needs to be as accurate as possible: indeed the precision of $\hat{\psi}$ strongly depends on these parameters). This fact allows one to have higher accuracy at the expenses of

more computation. One can indeed compute the estimates $(\hat{\varphi}, \hat{\theta}, \hat{\psi})$ corresponding to the four lowest local minima of $\mathcal{P}(k_\varphi, k_\theta)$, instead of the estimate $(\hat{\varphi}, \hat{\theta}, \hat{\psi})$ corresponding only to the lowest one, and decide about the best one simply by de-rotating the range image and checking the root-mean-square difference between them and the reference image. This provision, which ensures a precision of the angular parameter $(\hat{\varphi}, \hat{\theta}, \hat{\psi})$ within one degree, is useful only when the local minima of $\mathcal{P}(k_\varphi, k_\theta)$ are rather close. When they are far apart the lowest one can be trusted as best estimate.

The registration of 3-D views is a natural application of methods for estimating 3-D rigid motion. The performance of the proposed algorithm in this task is reported below. Fig.2-(a) and Fig.2-(b) show two partially overlapped range images of a bas-reliev by the Renaissance sculptor Donatello, belonging to the main altar of the Church of Sant'Antonio in Padova[2]. This object, whose dimension are approximately 60×100 cm, is very articulated since there are many anatomical details such as faces, arms, hands, etc., in full 3-D reliev.

The regions of the range images associated to the same scene were determined by a manual procedure and the proposed algorithm was used in order to determine the rotation and the translation between the taking positions of the range camera. Fig.2-(c) shows the composition of the range images of Fig.2-(a) and Fig.2-(b) based on the estimated rotation and translation, without any noise filtering. The result is truly hampered by the noise. Fig.2-(d) shows the composition of the same range data by the procedure applied to range images smoothed by a gaussian low-pass filter and decimated (for computational efficiency). Fig.3 shows the range data of Fig.2-(d) after a further averaging, which eliminates the visual effects of the one-degree misregistration of the angular parameters, inherent to the precision of the method, and considerably improves the visual quality of the registered data.

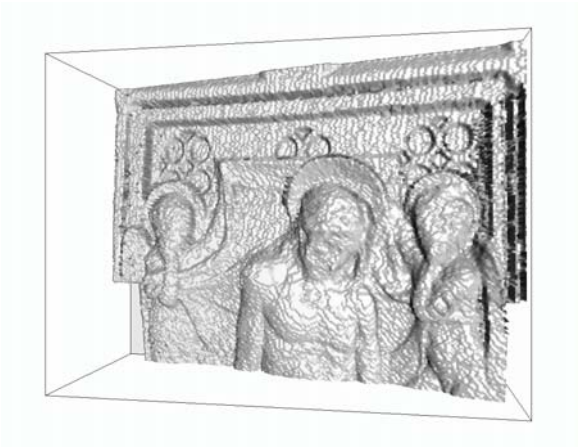

Figure 3: View of composition, after averaging.

[2]We acknowledge J. A. Beraldin of the Information Technology Group of NRCC-Ottawa and F. Bernier for the range data used in this work.

4. CONCLUSIONS

This work presents a new algorithm for estimating 3-D rotations and translations based on the frequency domain. It is suitable to give unsupervised estimates within 1° degree precision of the angular parameters and it can be applied to 3-D views registration in tasks where this precisions is adeguate or it can be used in order to obtain effective starting points for standard feature-based methods, which, as well-known, can give accurate solutions, once they are properly initiated [3].

Future work will aim to consolidate the robustness and the efficiency of the proposed 3-D registration technique by studying better ways of discriminating the local minimum of $\mathcal{P}(k_\varphi, k_\theta)$. An important aspect of the method, which is worth investigating, is the improvement on precision and robustness which one may gain by using texture information (easily obtainable by using also a digital photo-camera in the acquisition process) along with range data.

5. REFERENCES

[1] P.J. Besl and N.D. McKay, "A Method for Registration of 3-D Shapes", *IEEE Trans. on PAMI*, Vol. 14, No.2, pp. 239-259, Feb. 1992.

[2] S. Weik, "Registration of 3-D Partial Surface Models Using Luminance also and Depth Information", *Proc. of International Conference on Recent Advances in 3-D Digital Imaging and Modeling*, Ottawa, Canada, May 1997, pp. 93-100.

[3] H. Hügli, C. Schültz, "Geometric Matching of 3-D Objects: Assessing the Range of Successful Initial Configurations", *Proc. of International Conference on Recent Advances in 3-D Digital Imaging and Modeling*, Ottawa, Canada, May 1997, pp. 101-106.

[4] L. Lucchese, G. Doretto, G.M. Cortelazzo, "Frequency Domain Estimation of 3-D Rigid Motion Based on Range and Intensity Data", *Proc. of International Conference on Recent Advances in 3-D Digital Imaging and Modeling*, Ottawa, Canada, May 1997, pp. 107-112.

[5] L. Lucchese, G.M. Cortelazzo, C. Monti, "A Frequency Domain Technique for Estimating Rigid Planar Rotations", *Proc. of International Symposium on Circuits and Systems 96*, Atlanta, Georgia, May 1996, Vol. 2, pp. 774-777.

[6] L. Lucchese, G.M. Cortelazzo and C. Monti, "Estimation of Affine Transformations between Images Pairs via Fourier Transform", *Proc. of IEEE 1996 International Conference on Image Processing*, Lausanne, Switzerland, Sept. 1996, Vol. III, pp. 715-718.

[7] M. Rioux and L. Cournoyer, *The NRCC Three-dimensional Image Data Files*, Ottawa: National Research Council of Canada, June 1988.

[8] R. Bernardini, G.M. Cortelazzo, G.A. Mian, "A Sequential Multidimensional Cooley-Tukey Algorithm", *IEEE Trans. Signal Processing*, 42, pp. 2430-2438, Sept. 1994.

[9] R. Bernardini, G.M. Cortelazzo, G.A. Mian, "Unit Radix Graphs and Their Application to the Computation of MD FFT", submitted.